Molecular Orientation and Strain in Injection Moulding of Thermoplastics

R. Pantani, V. Speranza, A. Sorrentino and G. Titomanlio*

University of Salerno, dept. of Chemical and Food Engineering – I84084 Fisciano (SA) – ITALY

Summary: Obtaining reliable predictions for molecular orientation is currently one of most challenging targets in the simulation of the injection moulding process, being the starting point toward a better understanding of how crystallisation kinetics and final morphology are influenced by flow fields during processing. Although pressure and velocity distribution can be satisfactorily described by viscous models, the viscoelastic nature of the polymer needs to be accounted for in the description of molecular orientation evolution. In this work, different choices for the dumbbell model are adopted to describe the evolution of molecular orientation by effect of kinematics obtained by a viscous approach. Comparison with literature data of birefringence distributions in injection moulded disks identifies one of the choices which correctly describes main features of data.

Introduction

Molecular orientation consists in the preferential alignment of molecular chains along one particular direction, and it develops whenever either shear or elongational flows occur. In a plastic melt at rest, molecular segments are in a random state under maximum disorder; vice versa, during forming processes, by effect of flow, molecular chains are extended and aligned along a preferential direction: they assume a particular "orientation".

Orientation of molecular chains can often determine a marked anisotropy of the majority of final properties. Furthermore, molecular orientation and strain cause in semi crystalline polymers an enhancement of crystallisation kinetics for both thermodynamic and kinetic reasons [1]: an oriented melt has a higher free energy (and thus a higher melting point), and the kinetic barrier to overcome in the transition from the molten to the crystalline state lowers because extended chains are closer to their condition in the final crystal. A reliable description of the effect of flow on molecular orientation is therefore the starting point toward a better understanding of how crystallisation kinetics and final morphology are influenced by flow fields during processing.

Indeed, considerable attention has been given by researchers to the development of orientation in injection moulding of thermoplastics, and most of the work has been carried out on PolyStyrene, since for this material frozen-in birefringence can be easily used as a measure of orientation, being

 CCC 1022-1360/00/$ 17.50+.50/0

the contribution to birefringence of residual stresses negligible in the solid, due to the differences of optical coefficients between molten and glassy state [2]. The first attempt to predict orientation distribution in injection moulded PS samples is due to Isayev and Hieber [3], using Leonov viscoelastic constitutive equation. Following their basic work, most of the work focusing on simulation of molecular orientation has been carried out by using Leonov model [4] [5] [6].

Indeed, prediction of molecular orientation evolution does require the description of the viscoelastic nature of the polymer. On the other hand, as far as injection moulding is concerned, there is no need of a viscoelastic description of the material to obtain reliable pressure and velocity distributions [7] and indeed a full viscoelastic description of the process is difficult especially when complex geometries are considered. Therefore, in this work, simple viscoelastic models are applied to relate molecular orientation and strain to kinematics obtained parallelely by a viscous approach. Model results are validated by comparison with literature data of birefringence distributions in injection moulded PS disks [6] and are compared with literature simulations of the same data obtained with a complete viscoelastic approach based on Leonov model.

Modelling of molecular orientation

The elastic dumbbell model is one of the most simple schemes of description of polymer molecules [8]. In spite of its simplicity, it is able to describe orientation and stretching of molecules due to a flow field, and many of the main features of the rheological behaviour of a polymer melt can be reproduced (at least qualitatively) by this model, once an appropriate choice of the relaxation time is identified.

The constitutive equation for elastic dumbbells can be written as

$$\frac{D}{Dt}\underline{\underline{A}} - \underline{\underline{\nabla v}}^T \cdot \underline{\underline{A}} - \underline{\underline{A}} \cdot \underline{\underline{\nabla v}} = -\frac{1}{\tau}\left(\underline{\underline{A}} + \underline{\underline{\nabla v}} + \underline{\underline{\nabla v}}^T\right) \qquad (1)$$

where

$$\underline{\underline{A}} = 3\left(\langle \underline{R}\,\underline{R} \rangle - \langle \underline{R}\,\underline{R} \rangle_0\right) \Big/ \langle R_0^2 \rangle \qquad (2)$$

$\underline{R}$ being the end-to-end vector of a single dumbbell and the symbol $< >$ standing for the average over the configuration space. The second order tensor $\underline{\underline{A}}$ is a measure of the "deformation" of a dumbbell population with respect to the rest equilibrium state $\langle \underline{R}\,\underline{R} \rangle_0$ when the stress tensor is zero, and the dumbbell length is $\langle R_0^2 \rangle$.

According to the derivations of Kuhn and Grün[9], the tensor $\underline{\underline{A}}$ is proportional to the refractive index tensor. Therefore, in this work, the maximum eigenvalue of the tensor $\underline{\underline{A}}$, which usually is much larger than the others and is referred to as ϕ in the following, was used as an index of molecular orientation, directly proportional to birefringence. It can be worth mentioning that the maximum molecular strain λ (i.e. the strain along the direction of maximum molecular orientation) is related to ϕ by the equation:

$$\lambda = \sqrt{\phi + 1} \qquad (3)$$

Description of molecular deformation by means of equation 1 does not limit the length of the end-to-end vector, namely of chain elongation; however, starting from rest, when according to molecular theories the average distance between the ends of macromolecules is $\ell\sqrt{\nu}$ (where ℓ and ν are length and number of Kuhn elements per chain), the maximum value of molecular strain λ should not overcome $\sqrt{\nu}$. For most polymers λ_{max} is of the order of 10 (depending on material molecular weight of the repeating unit and on the number of backbone atoms per structural units [10]) and it is, therefore, expected that ϕ could be maximum of the order of one hundred or a few hundreds.

Once velocity field is known, equation 1 presents a single parameter, the relaxation time, τ. In classical linear elastic dumbbell model, the relaxation time is taken as constant. However equation 1 is often used in the same form also when the relaxation time is not constant, leading to nonlinear dumbbell models[11]. In this work, different options for the choice of τ are tested, with the aim of verifying which one leads to best results in term of molecular orientation and strain frozen in the final object after processing.

Option "a": relaxation time function of temperature, only

The first possibility (option "a") is to keep τ constant with shear rate, in agreement to standard elastic dumbbell's theories. In such a case, the relaxation time ($\tau=\tau_0$) can be assumed to be a function of temperature and pressure, only. Ignoring for the moment the effect of pressure, dependence upon temperature can be described by a WLF equation as

$$\tau_0(T) = \tau^* 10^{-\frac{A_1(T-T_0)}{A_2+T-T_0}} \qquad (4)$$

where the values of constants A_1, A_2 and T_0 can be drawn from viscosity shift factor. The value of τ^* can be determined by several procedures which give values close to each other; in this work it was determined as the inverse of the lowest frequency at which the loss modulus, G', equals the

storage modulus, G" at the reference temperature T_0.

According to the Dumbbell model, the shear viscosity, η, for a steady-state shear flow, can be calculated as [8]

$$\eta = G\tau \qquad (5)$$

where G is the shear modulus.

If G is a constant and τ is equal to τ_0 in equation 5, under constant temperature η is also a constant, i.e. according to the model it should not depend upon shear rate. Adopting option "a" leads thus to the impossibility of describing polymers shear thinning behaviour.

Option "b": relaxation time is function of shear rate parallelely to viscosity

The second possibility (option "b") is to expressly keep into account equation 5 in the definition of τ.

As experiments show that η is function of T and $\dot{\gamma}$, if G is assumed constant in equation 5, τ must be function of temperature and shear rate. In particular, in this work, the following Cross equation

$$\tau(T,\dot{\gamma}) = \frac{\tau_0(T)}{1+\left[\frac{\tau_0(T)\dot{\gamma}}{k}\right]^{1-n}} \qquad (6)$$

was adopted, where τ_0 can again be described by equation 4. According to this second option, relaxation time changes with temperature and shear rate parallelely to viscosity, as shear modulus is assumed constant in equation 5.

Option "c": relaxation time is function of shear rate according to a viscoelastic characterisation

The third possible option (option "c") is to perform a full viscoelastic characterisation of the polymer, and to consider that for a steady-state shear flow the dumbbell model predicts, together with equation 5, also the first normal stresses difference as [8]

$$N_1 = 2G\tau^2\dot{\gamma}^2 \qquad (7)$$

and, substituting equation 5 into equation 7

$$N_1 = 2\eta\tau\dot{\gamma}^2 \qquad (8)$$

As experiments show that both η and N_1 are function of shear rate, equation 8 allows to identify the dependence of τ on shear rate based on the measurements of η and N_1 during steady-state shear flow. Alternatively, if material characterisation is performed on the basis of oscillatory data of loss, G", and storage, G', moduli, $\eta(\dot{\gamma})$ can be determined by adopting the Cox-Merz rule

$$\eta(T,\dot{\gamma}) = \frac{G''(T,\omega)}{\omega}\left[1+\left(\frac{G'(T,\omega)}{G''(T,\omega)}\right)^2\right]^{0.5}\Bigg|_{\omega=\dot{\gamma}} \quad (9)$$

and $N_1(\dot{\gamma})$ can be determined by adopting the empirical Laun's [12] rule

$$N_1(T,\dot{\gamma}) = 2G'(T,\omega)\left[1+\left(\frac{G'(T,\omega)}{G''(T,\omega)}\right)^2\right]^{0.7}\Bigg|_{\omega=\dot{\gamma}} \quad (10)$$

On the basis of equation 8, and consistently with equations 9 and 10, the relaxation time can be obtained from loss and storage moduli G" and G'. Thus, from equations 8, 9 and 10, it is obtained as

$$\tau(T,\dot{\gamma}) = \frac{G'(T,\omega)}{\omega G''(T,\omega)}\left[1+\left(\frac{G'(T,\omega)}{G''(T,\omega)}\right)^2\right]^{0.2}\Bigg|_{\omega=\dot{\gamma}} \quad (11)$$

This third option (option "c") normally provides a different description of the effect of flow on relaxation time, τ, with respect to option "b". As reported in [10], if relaxation time is taken from independent measurements of normal stresses difference and viscosity, it starts to decrease at lower shear rates with respect to η, and assumes a dependence upon shear rate higher than that of viscosity. This means that, even if equations 4 and 6 can still be adopted to describe relaxation time as a function of shear rate, parameters k and n in equation 6 are different from those adopted in option "b".

Birefringence distribution in injection moulded disks

In a recent paper, Kwon and co-workers[6] presented data of birefringence distribution along thickness at different radial positions in centrally injected PS moulded disks (diameter 102mm, thickness 2.01mm, packing pressure 16.5MPa, packing time 6s).

Data are reported in figure 1 and show interesting features: starting from sample skin at each radial position birefringence reaches a relative maximum (due to filling flow) at about 20%-25% of sample half thickness (these maxima will be referred to in the following as "F"); on increasing distance from sample skin, birefringence first fades down and then increase again at about 50% of sample half thickness where a new relative maximum due to the packing flow is reached (these second maxima will be referred to in the following as "P"). On increasing distance from the gate, lower birefringence values are found: maxima "F" are higher at positions closer to the gate because for the same flow rate

average velocity is higher at smaller radial positions; also maxima "P" are higher the smaller is the distance from the gate for the same geometrical reason and in addition because packing flow (essentially dictated at each positions by the densification of material downstream to the position considered) is larger closer to the gate.

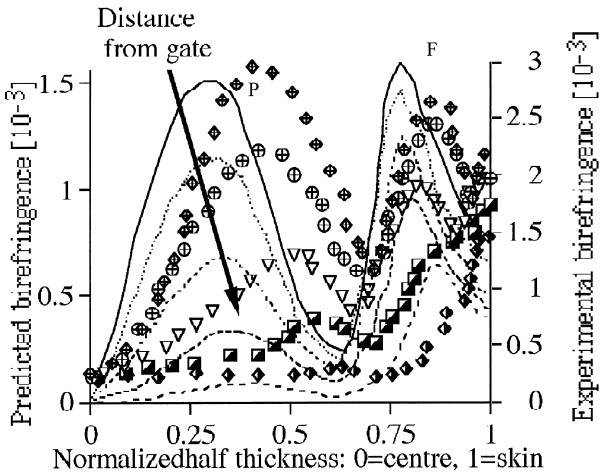

Figure 1. Comparison between experimental data and predictions as obtained by Kwon and co-workers[6]. Radial positions: r=17.5mm, 22.5mm, 30mm, 37.5mm, 45mm

It has to be pointed out that packing flow is much less intense than filling flow. In spite of this, experimental data of figure 1 show that, almost at each radial positions, both flows are equally effective in orienting molecules. This is reasonably due to the fact that filling flow induces an orientation on molecules at high temperatures (when relaxation time is short), whereas packing flow acts on molecules at much lower temperatures (even close to solidification) and thus when relaxation times are much longer. Birefringence distributions reported by Kwon and co-workers[6] therefore reveal that for the moulding conditions analysed, flow and temperature effects are almost perfectly balanced. Therefore, predicting such an orientation distribution is a challenging test for a simulation code.

It can finally be noticed that highest value of birefringence reported by Kwon and co-workers[6] is about 50 times smaller than the maximum value of birefringence for PS (which is about 0.12[2]), i.e. experimental values found for birefringence indicate a low level of orientation. It is therefore

expected that the values of orientation parameter ϕ for tests reported in Kwon et al. [6] should be fifty times smaller than the maximum value of ϕ which, as mentioned in the previous section, is expected to be a few hundreds. this leads to values of ϕ of the order of 10.

A 2-mode Leonov viscoelastic model with a WLF shift factor for temperature was adopted in Kwon and co-workers to perform simulations of birefringence distribution. In particular, data were compared with predictions obtained by adopting a viscoelastic approach (based on Leonov model) for both kinematics and orientation. Apart from a scale factor (predicted values of birefringence were lower than experimental ones), comparison was satisfactory, as shown in figure 1. In particular, main features of experimental data were correctly reproduced, such as the presence of the two maxima, having about the same values of birefringence.

Discussion

Relaxation time and viscosity from Leonov description

In order to describe material viscoelastic properties according to Dumbbell model, and in particular adopting the three options listed in the modelling section above, it is necessary to have information about material viscosity and first normal stresses difference, or about storage and loss moduli. Being data on the material used by Kwon and co-workers[6] not available, in this work the material description performed by Kwon and co-workers[6] on the basis of Leonov model was adopted to generate the material functions G' and G".

Indeed, from a generic n-mode Leonov model, it is possible to rebuild the curves of storage and loss moduli versus frequency according to the equations

$$G'(T,\omega) = \sum_{k=1}^{n} \frac{\eta_k \theta_k \alpha(T) \omega^2}{1 + \omega^2 \theta_k^2 \alpha(T)^2} \qquad (12)$$

$$G''(T,\omega) = \eta_0 s \alpha(T) \omega + \sum_{k=1}^{n} \frac{\eta_k \alpha(T) \omega}{1 + \omega^2 \theta_k^2 \alpha(T)^2} \qquad (13)$$

where η_k , θ_k and s are constants of the Leonov model and $\alpha(T)$ is a WLF type thermal shift factor. All these parameters were reported by Kwon and co-workers[6]

Values of viscosity calculated by means of equation 8 (adopting equations 12 and 13 to describe moduli dependence on temperature and frequency) were used as data for a best fit procedure, identifying the parameters of a Cross-WLF equation

$$\eta(\dot{\gamma},T)=\frac{\eta_0(T)}{1+\left(\frac{\eta_0(T)}{m}\dot{\gamma}\right)^{1-q}} \qquad (14)$$

where

$$\eta_0(T)=\eta^*10^{-\frac{B_1(T-T_0)}{B_2+T-T_0}} \qquad (15)$$

which was used to describe material viscosity in this work. The best fitting values of the parameters of equations 14 and 15 are reported in table 1.

Similarly, values of moduli calculated by means of equations 12 and 13 were used to identify the parameters of equations 4 and 6 which describe relaxation time according to the different options adopted in this work.

In particular, equating equations 12 and 13 at T_0=220°C, a reference value of τ^*=0.035s was identified. Constants B_1 and B_2 of equation 15 complete the definition of the thermal shift factor for relaxation time according to option "a" (A_1 and A_2 of equation 4 can be set equal to B_1 and B_2 of equation 15). If option "b" is adopted (τ versus shear rate runs parallelely to η), parameters of equation è are linked to those found for viscosity (equation 14): in particular n (flow index) has the same value of q and $k=m\tau^*/\eta^*$. Values of parameters for equation 4 (thermal shift factor and τ^*), are the same as for option "a".

As far as option "c" is concerned, equations 11, 12 and 13 were adopted to find the dependence of τ on shear rate. Calculated values were treated as data for a best fit procedure, identifying the parameters of equation 6. Best fitting parameters are reported in table 2. Thermal shift factors resulted to be nearly the same as that found for options "a" and "b", therefore the same parameters were used in equation 4 for all options adopted.

A plot of dependence of relaxation time upon shear rate is shown in figure 2 for all options considered in this work. According to option "c", relaxation time at low shear rates asymptotises to a plateau higher than relaxation time identified by options "a" and "b", and decreases from this plateau at shear rates lower with respect to option "b" (and thus with respect to viscosity); at high shear rates it decreases with a dependence upon shear rate steeper than that of viscosity. After equation 5, this result implies that shear modulus G is also dependent upon $\dot{\gamma}$ and in particular it increases on increasing shear rate [10] and thus on increasing molecular strain. This result is therefore similar to that imposed by adopting a FENE dumbbell model.

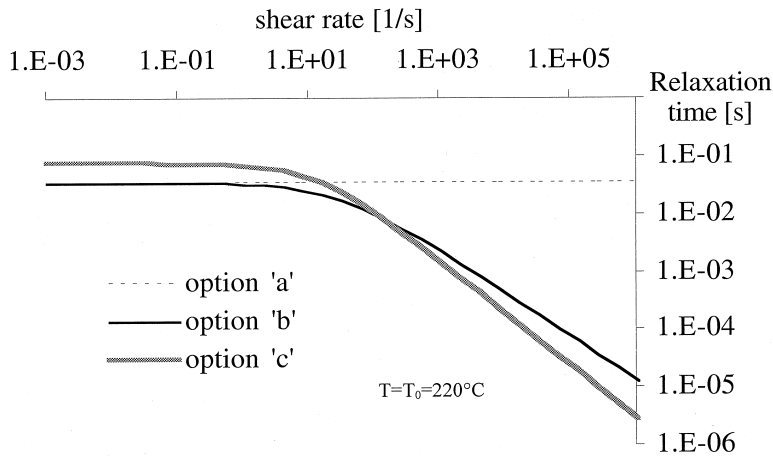

Figure 2. Dependence of relaxation time on shear rate (at $T=T_0=220°C$) according to the three different options adopted in this work.

Table 1: Parameters used in equations 14 and 15 to describe material viscosity

η_0 [s]	900
T_0 [°C]	220
B_1 [-]	4.5
B_2 [°C]	181.06
m [Pa]	31000
q [-]	0.252

Table 2: Parameters used in equations 4 and 6 to describe material relaxation time according to the different options adopted in this work

	option "a"	option "b"	option "c"
τ_0 [s]	0.036	0.036	0.075
T_0 [°C]	220	220	220
A_1 [-]	4.5	4.5	4.5
A_2 [°C]	181.06	181.06	181.06
k [-]		1	1
n [-]		0.252	0.1

Modelling of the moulding test

The moulding test presented by Kwon and co-workers[6] (centrally injected PS moulded disks of diameter 102mm and thickness 2.01mm, packing pressure 16.5MPa, packing time 6s) was simulated by means of a software code developed at University of Salerno. Details regarding both field equations and constitutive equations adopted in the code are given elsewhere [7] [13].

In this work we focus the attention on birefringence (orientation) predictions. To this purpose, exactly the same description of material PVT behaviour and thermal properties as used by Kwon and co-workers[6] were adopted. Furthermore, the same boundary conditions were adopted for field equations, that is

- no-slip condition at the cavity wall
- constant polymer temperature at the cavity wall, equal to mould wall temperature (Dirichlet boundary condition)
- symmetric conditions at the cavity centre plane;

Simulated temperature profiles resulted to be quite similar to those reported by Kwon et al. [6]: comparison is reported in figures 3 and 4 which refer to the end of filling step (0.67s) and the end of packing (6.7s), respectively.

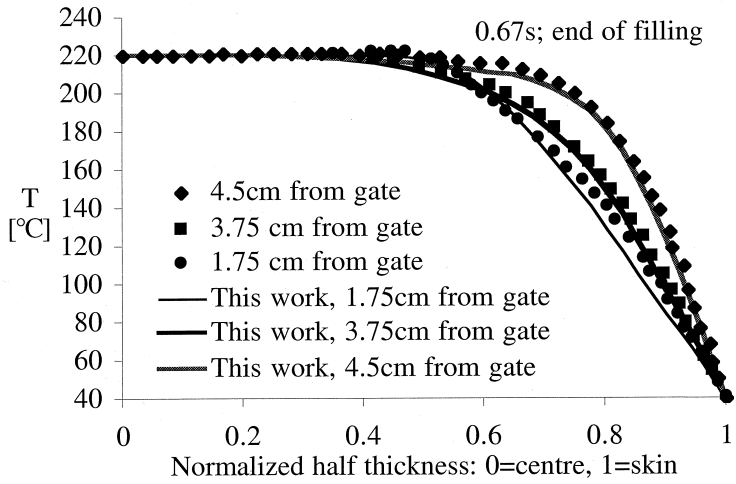

Figure 3. Comparison between temperature profiles obtained in this work and those reported by Kwon and co-workers[6] at the end of filling step

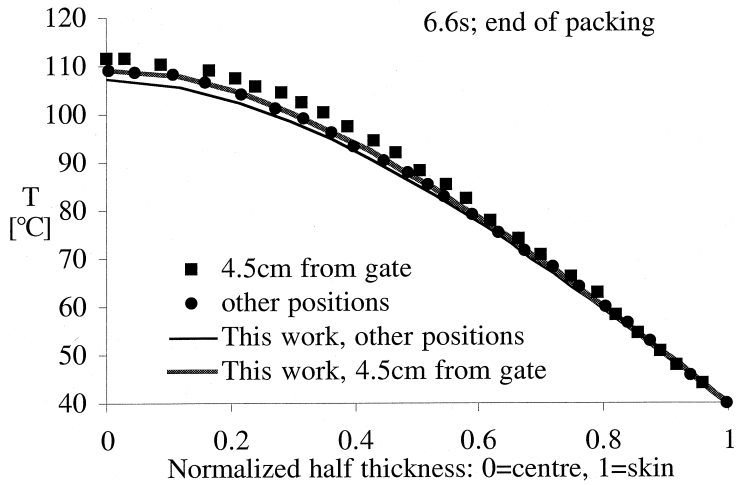

Figure 4. Comparison between temperature profiles obtained in this work and those reported by Kwon and co-workers[6] at the end of packing step.

Prediction of birefringence distribution

The first attempt to simulate data reported by Kwon and co-workers regarding birefringence distribution inside the moulding was performed by adopting option "a" (τ depending on temperature, only). Results are shown in figure 5, where calculated values of orientation parameter ϕ

are compared with experimental birefringence distribution.

Comparison is poor, also on a qualitative basis: maxima "P" (due to packing flow) are highly underpredicted with respect to maxima "F" (due to filling flow), and even hardly detected on the plot. Furthermore, orientation parameter ϕ reaches values as high as 8000, far over the expected value (of the order of about 10) and also beyond the maximum reachable value that, as mentioned in the modelling section above, should be of the order of a few hundreds. Such high values are obviously due to the fact that, during mould filling, deformation gradients are high (shear rates of the order of $1000s^{-1}$) and relaxation time is a constant of the order of 0.01s (very high if compared to the shear rate). Therefore equation 1 becomes unbalanced toward a tremendous increase of orientation during the whole filling step.

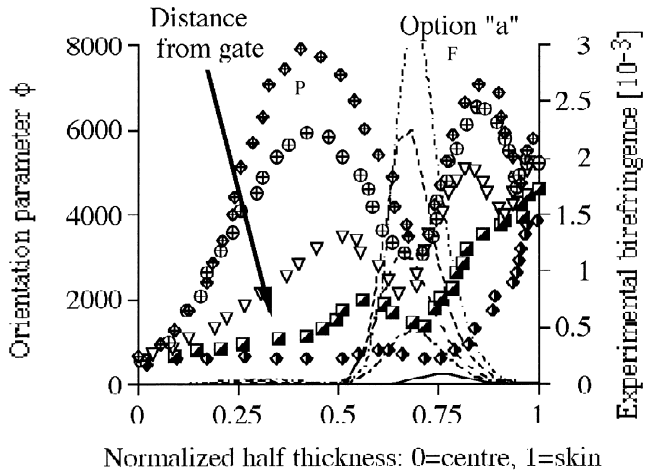

Figure 5. Comparison between experimental data reported by Kwon and co-workers[6] (symbols) and predicted results obtained in this work adopting option "a" (lines). Radial positions: r=17.5mm, 22.5mm, 30mm, 37.5mm, 45mm

Option "b", which adopts a decrease of τ during filling (at high shear rates) parallel to viscosity, is expected to improve simulation results. Indeed, as shown in figure 6, calculations performed by adopting option "b", even if still unsatisfactorily also from a qualitative point of view, produce two considerable improvements with respect to option "a":

- heights of maxima "P" (due to packing flow) reach values which are comparable to those of maxima "F" (due to filling flow);

- values of orientation parameter are within the limit of a few hundreds and close to the value of about 10 which was estimated on the basis of birefringence values.

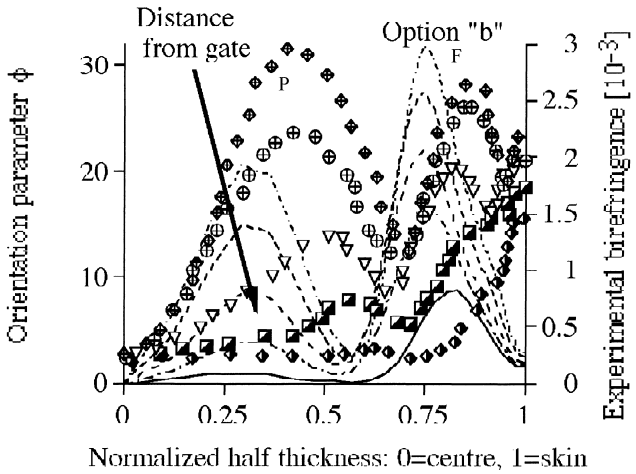

Figure 6. Comparison between experimental data reported by Kwon and co-workers[6] (symbols) and predicted results obtained in this work adopting option "b" (lines). Radial positions: r=17.5mm, 22.5mm, 30mm, 37.5mm, 45mm

Results of simulation performed by adopting option "c" are shown in figure 7. Comparison with birefringence experimental data is satisfactory: maxima "F" and "P" reach about the same levels, as shown by data, and values of orientation parameter ϕ are correctly below the estimated limit of 10, indicating a value of molecular strain of about 3, which is in line with low values found for birefringence.

Furthermore, results of simulations shown in figure 7 favourably compare (at least qualitatively) also with results obtained by adopting Leonov viscoelastic model for both kinematics and residual stresses (birefringence) (reported in figure 1) thus validating the whole logical path applied in this work.

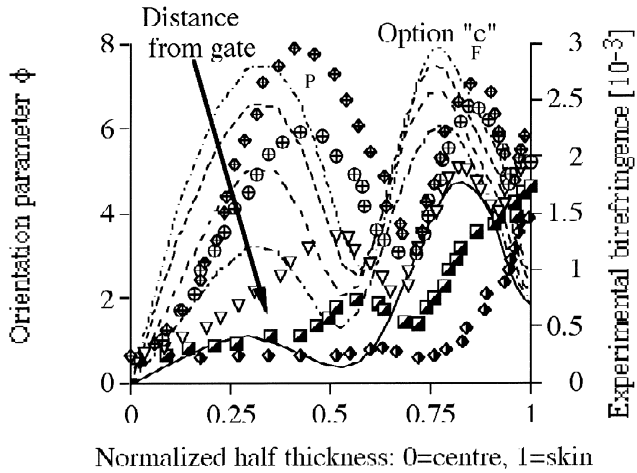

Figure 7.Comparison between experimental data reported by Kwon and co-workers[6] (symbols) and predicted results obtained in this work adopting option "c" (lines). Radial positions: r=17.5mm, 22.5mm, 30mm, 37.5mm, 45mm

Conclusions

In this work, dumbbell models were adopted to describe the evolution of molecular orientation in injection moulding process by effect of kinematics obtained by a viscous approach

Three options for relaxation time were tested to describe birefringence distributions in PS injection moulded disks (data taken from literature[6]). Best results (also in terms of molecular strain) were obtained relating dependence of relaxation time upon shear rate to that of both viscosity and first normal stresses difference. With this option (option "c") a stronger dependence of relaxation time upon shear rate is obtained with respect to that shown by viscosity.

Prediction of final distribution of molecular orientation in injection mouldings reproduces all relevant features shown by the data, similarly to predictions based on a full viscoelastic Leonov model of the process.

On the basis of these results, it can be concluded that, if an appropriate choice of relaxation time is adopted, the dumbbell model provides a reliable description of the evolution of molecular orientation and, on the basis of appropriate kinematics and solidification criterion, of final orientation distribution after processing.

[1] A Keller and HWH Kolnaar, "*Flow-induced orientation and structure formation* in *Processing of Polymers"* edited by HEH Meijer, vol. 18 of *"Materials Science and Technology: A Comprensive Treatment"* VCH, **1997**

[2] LCE Struick, "*Internal stresses, Dimensional instabilities and molecular orientations in plastics"*, Wiley and sons, **1990**
[3] AI Isayev, CA Hieber, *Rheol. Acta,* **1980**, *19*, 168
[4] H Mavridis, AN Hrymak, J Vlachopoulos, *J. Rheol*, **1988**, *32*, 639
[5] TAM Flaman, "*Build-up and relaxation of molecular orientation in injection moulding"*, PhD Thesis, TU Eindhoven, **1990**
[6] IH Kim, SJ Park, ST Chung, TH Kwon, *Polym. Eng. Sci.*, **1999**, *39*, 1930
[7] R Pantani, V Speranza, G Titomanlio, *Polym. Eng. Sci.,* **2001**, *41*, 2022
[8] RB Bird, CF Curtiss, RC Armstrong, O Hassager *"Dynamics of Polymeric Liquids"*, vol. 2, J. Wiley and Sons, **1987**
[9] W Kuhn, F Grün, *Kolloid-Z*, **1942**, *101*, 248
[10] DW Van Krevelen, "*Properties of Polymers"*, Elsevier, **1990**
[11] G Marrucci, *J. Non-Newtonian Fluid Mech*, **1996**, *62*, 279
[12] HM Laun, *J.Rheol*, **1986**, *30*, 459
[13] G Titomanlio, V Speranza, V. Brucato, *Int. Polym. Proc.* **1995**, *10*, 55